Article:
Califano, M (2015) Origins of Photoluminescence Decay Kinetics in CdTe Colloidal Quantum Dots. ACS Nano, 9 (3). pp. 2960-2967. ISSN: 1936-0851

https://doi.org/10.1021/nn5070327

Origins of Photoluminescence Decay Kinetics in CdTe Colloidal Quantum Dots

Marco Califano *

Institute of Microwaves and Photonics, School of Electronic and Electrical Engineering, University of Leeds, Leeds LS2 9JT, United Kingdom

E-mail: m.califano@leeds.ac.uk

Abstract

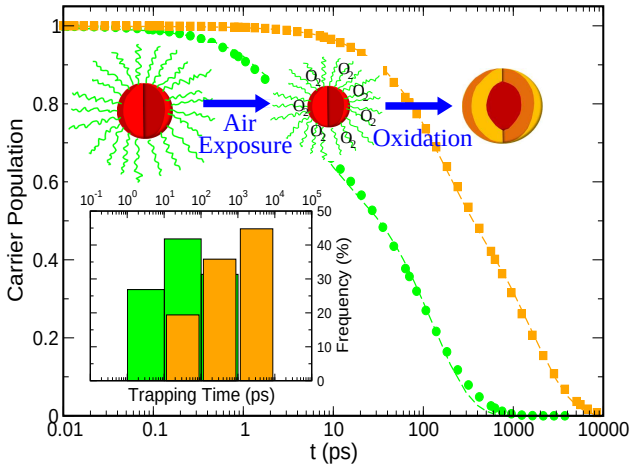

Recent experimental studies have identified at least two non-radiative components in the fluorescence decay of solutions of CdTe colloidal quantum dots (CQDs). The lifetimes reported by different groups, however, differed by orders of magnitude, raising the question of whether different types of traps were at play in the different samples and experimental conditions and even whether different types of charge

*To whom correspondence should be addressed

carriers were involved in the different trapping processes. Considering that the use of these nanomaterials in biology, optoelectronics, photonics and photovoltaics is becoming widespread, such a gap in our understanding of carrier dynamics in these systems needs addressing. This is what we do here. Using the state-of-the-art atomistic semiempirical pseudopotential method we calculate trapping times and non-radiative population decay curves for different CQD sizes considering up to 268 surface traps. We show that the seemingly discrepant experimental results are consistent with the trapping of the hole at unsaturated Te bonds on the dot surface in the presence of different dielectric environments. In particular, the observed increase in the trapping times following air exposure is attributed to the formation of an oxide shell on the dot surface which increases the dielectric constant of the dot environment. Two types of traps are identified, depending on whether the unsaturated bond is single (type I) or part of a pair of dangling bonds on the same Te atom (type II). The energy landscape relative to transitions to these traps is found to be markedly different in the two cases. As a consequence the trapping times associated with the different types of traps exhibit a strikingly contrasting sensitivity to variations in the dot environment. Based on these characteristics, we predict the presence of a sub-ns component in all PL decay curves of CdTe CQDs in the size range considered here, if both trap types are present. The absence of such a component is attributed to the suppression of type-I traps.

KEYWORDS: trapping, surface, Auger processes, nanocrystals, colloidal quantum dots, pseudopotential method

Carrier dynamics at the surface of colloidal quantum dots (CQDs), although of great importance for their technological application, is still poorly understood. It is well known that the incomplete saturation of the dangling bonds at their surface achieved by conventional organic ligands leads to the formation of trap states that can localise charge carriers, degrading device performance. However the details of the trapping dynamics in many materials are still subject of debate and intense research.[1–19] In particular, in some cases

it is even unclear whether it is the trapping of the electron and/or that of the hole that affects the fluorescence efficiency, as several non-radiative decay components have been observed with different magnitudes (sometimes differing by several orders of magnitude for the same material), prompting the suggestion that different types of traps must be present. This is the case of CdTe CQDs, where recent experimental studies have evidenced fluorescence decay curves that required at least a tri-exponential function to yield good agreement with the observed kinetics.[17–19] In addition to radiative decay, two non-radiative components were therefore extracted from the experimental data, suggesting the presence of (at least) two types of traps. However their nature (i.e., whether hole or electron traps) was not clear[18] and their location on the surface was not determined. Furthermore the lifetimes extracted by different groups ranged from a few ps[17] to a few ns,[19] depending on the experimental conditions. The origin of the two non-radiative decay components remains therefore controversial. In principle both electron and hole traps can be present on the CQD surface. However, it is well known that organic ligands commonly used in the synthesis of CdTe, such as thiols, amines, and phosphonic and mercaptopropionic acids, bind to surface Cd atoms,[20] leaving most surface Te atoms undercoordinated.[21] These unsaturated Te bonds have been identified as hole traps by optically detected magnetic resonance,[21] and their energy location within the lower half of the CdTe band gap was confirmed by electrochemical studies.[22] Furthermore, high-resolution photoelectron spectroscopic studies[23] have revealed that lowly luminescent CQDs have a larger amount of surface Te atoms compared to highly luminescent ones. It is therefore reasonable to assume that the majority of active traps present on the surface of CdTe CQDs will be intra-gap hole traps associated with unsaturated Te bonds.

Here we present a detailed study of hole trapping at the surface of CdTe CQDs of different sizes and in different environments, using LDA-quality wave functions, obtained within the atomistic semiempirical pseudopotential method.[25] We find that there are indeed two kinds of hole traps, in agreement with the observation of two non-radiative

components in the fluorescence decay. We also show that the seemingly contrasting values of their lifetimes, observed in different experiments by different groups so far, can be rationalised when properly accounting for the characteristics of the different surface terminations and dielectric environments of the samples, and assuming an Auger mediated trapping mechanism[24] recently employed to explain the charge dynamics observed in CQDs of different materials and configurations, including CdSe cores,[13] InAs/ZnSe core/shell and impurity-doped CdSe:Te structures.[14]

Auger mediated trapping (AMT)[13,14,24] is a non-radiative decay process first suggested by Frantsuzov and Marcus[24] as a possible explanation of blinking in CQDs, in which the energy of the hole transition from a core-delocalised state to a localised state in the gap is transferred to the photogenerated conduction band edge electron promoting it to another core-delocalised state at a higher energy (see Figure 1). For an accurate

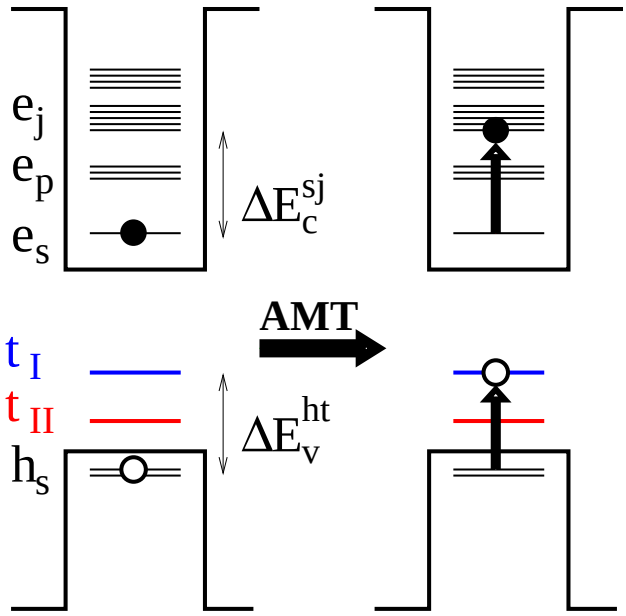

Figure 1: Schematics of the Auger-mediated trapping mechanism considered in this work. The energy ΔE_v^{ht} of the hole transition $|h_s \rightarrow t_n>$ from the band edge h_s to the intra-gap trap site t_n (n =I or II) is transferred non-radiatively to the core band edge s-like electron, which is promoted into one of the excited core states j, situated ΔE_c^{sj} higher in energy.

description of this process, which involves trap states with typical localization lengths of the order of a few interatomic distances, an atomistic approach is therefore indispens-

able. In this work the semiempirical pseudopotential method[25] - a state-of-the-art atomistic approach - is used. This approach was recently employed to accurately describe both hole[13,14] and electron dynamics[15] observed in different nanoscopic materials.

RESULTS AND DISCUSSION

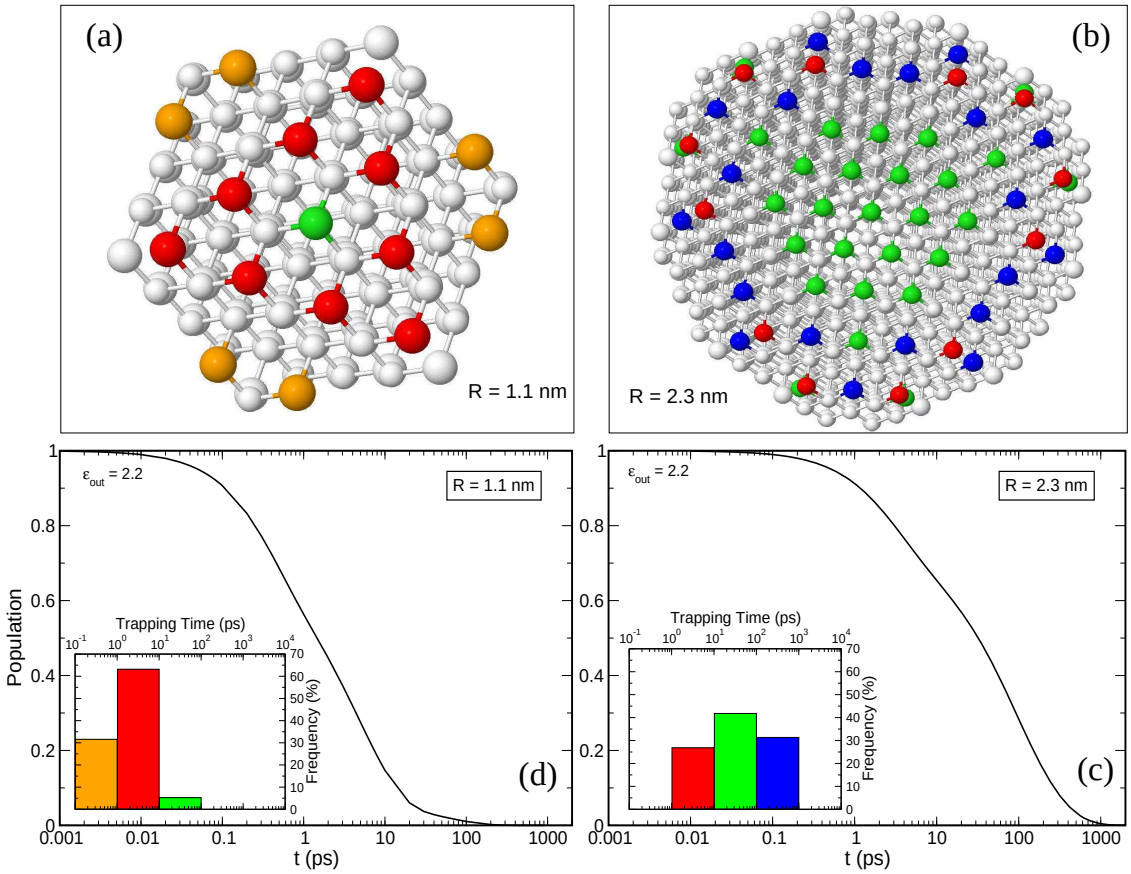

Figure 2: Surface trapping in CdTe CQDs of two different sizes. (a-b) Atomistically accurate position-resolved map of the AMT times calculated, for a CdTe CQD with R=1.1 nm (a) and 2.3 nm (b), by removing a single passivant at a time from the surface Te atoms indicated by the coloured spheres. For clarity Cd and Te atoms are shown in white whereas Cd and Te passivants are not displayed. (c-d) Corresponding non-radiative population decay curves, calculated considering the contribution of 76 (d) and 268 (c) surface traps. (c-d) Insets: Distribution of calculated hole transfer times to traps located at the surface in CdTe CQDs with R=2.3 nm (c) and R=1.1 nm (d). The color coding reflects the traps positions in (a-b).

There are, respectively, 76 and 268 Te dangling bonds on the surface of CdTe CQDs

with R=1.1 and 2.3 nm. Exploiting the tetrahedral symmetry of the underlying zinc-blende crystal structure, they can be reduced to only 5 and, respectively, 14 inequivalent traps, each of which can represent 4n ($n = 1$, 3 or 6) equivalent sites (see Figure 2a,b). For both sizes considered, such traps are centered around two different energy values (E_I and E_{II}) within the band gap (see Figure 1), depending on whether the trap is obtained from a single (I) or a double (II) dangling bond: [a] $E_I \approx E_{\mathrm{VBM}}^{\mathrm{bulk}} + 0.450$ eV and $E_{II} \approx E_{\mathrm{VBM}}^{\mathrm{bulk}} + 0.050$ eV (where $E_{\mathrm{VBM}}^{\mathrm{bulk}}$ is the position of the VBM of bulk CdTe).

The calculated distributions of the AMT times to these hole traps are presented in the insets of Figure 2c and d for the two different sizes. They are very narrow if compared to those characteristic for CdSe dots,[13,14] with the trapping times distributed over about 2 decades for both sizes, ranging from a few ps to a few hundreds of ps for the largest dot, in broad agreement with the distribution of the non-radiative lifetimes extracted by Boehme *et al.*[17] from the decay kinetics of CdTe CQD dispersions of different sizes (and identified as charge carrier trapping times), and similarly to the distributions found for InAs/ZnSe CQDs.[11,14] As already discussed in that case,[14] this is a common feature of the zinc-blende crystal structure compared to wurtzite, which leads to a larger number of equivalent sites on the surface (see Figure 2), hence a smaller spread in trapping times.

Table 1: CdTe trapping times: Comparison of theory and experiment. Comparison of the fast (τ_1) and slow (τ_2) components extracted from the fits to the experimental[17] and theoretical data for different CQD sizes (in this Table we follow the notation by Boehme *et al.* where τ_f is called τ_1 and τ_s τ_2). The rms error on the theoretical values is about 0.5%. The experimental data have been attributed to *electron* trapping,[17] whereas the theoretical data refer to *hole* trapping.

Diameter [nm]	τ_1 [ps]	τ_2 [ps]	data type	carrier
2.2	0.5	7.1	theory	hole
3.7	2.8±0.1	46±2	exp.	el.
4.6	4.6	125.5	theory	hole
6.3	192±34	942±2	exp.	el.

A more detailed comparison with the experimental data by Boehme *et al.* is provided

[a] Only one unsaturated bond was present on the whole surface for each calculation.

in Table 1, where the theoretical lifetimes were obtained following a similar procedure to the experimental case, i.e., by fitting with a bi-exponential function the theoretical population decay curve (as shown in Figure 3 for $R = 2.3$ nm). The latter (Figure 2c, d) was calculated as a sum of N exponentials [b] corresponding to the N different inequivalent traps ($N = 5$ for CQDs with $R = 1.1$ nm, and $N = 14$ in the case of $R = 2.3$ nm - see above),

$$P(t) = \sum_{i=1}^{N} w_i e^{-\frac{t}{\tau_i}}$$

where each weight w_i is given by the number $n(\tau_i)$ of equivalent sites on the surface with the specific trapping time τ_i (see Figure 2b)

$$w_i = n(\tau_i) / \sum_{i=1}^{N} n(\tau_i).$$

The theoretical decay times extracted with this procedure (Table 1) are in good agreement with the experimental estimates (attributed to electron trapping)[17] for both sizes considered, and correctly reproduce the observed trend with size. The question therefore arises of whether the experimental data might have been due to *hole*, rather than electron, trapping. Indeed, it needs to be pointed out that the experimental lifetimes used for comparison here are relative to CQD *dispersions*. Different results (i.e., much faster trapping times) were in fact obtained in the case of CQD *films* (for which the capping molecules, the inter-dot spacings and the dielectric environment were completely different), which were unambiguously attributed to the trapping of the *electron* through a combination of transient absorption and electrochemical gating measurements.[17] The evidence presented in support of electron, rather than hole, trapping in *dispersions*, was instead based uniquely on transient absorption measurements, and was therefore less conclusive: they observed a fast decay of the bleach signal relative to the $1S_{3/2}1S_e$ transition, which indicates a fast

[b] As the calculated trapping rates are much larger than those due to radiative recombination, the contribution of the latter process to the decay curve would only add a constant background on these time scales and has been neglected.

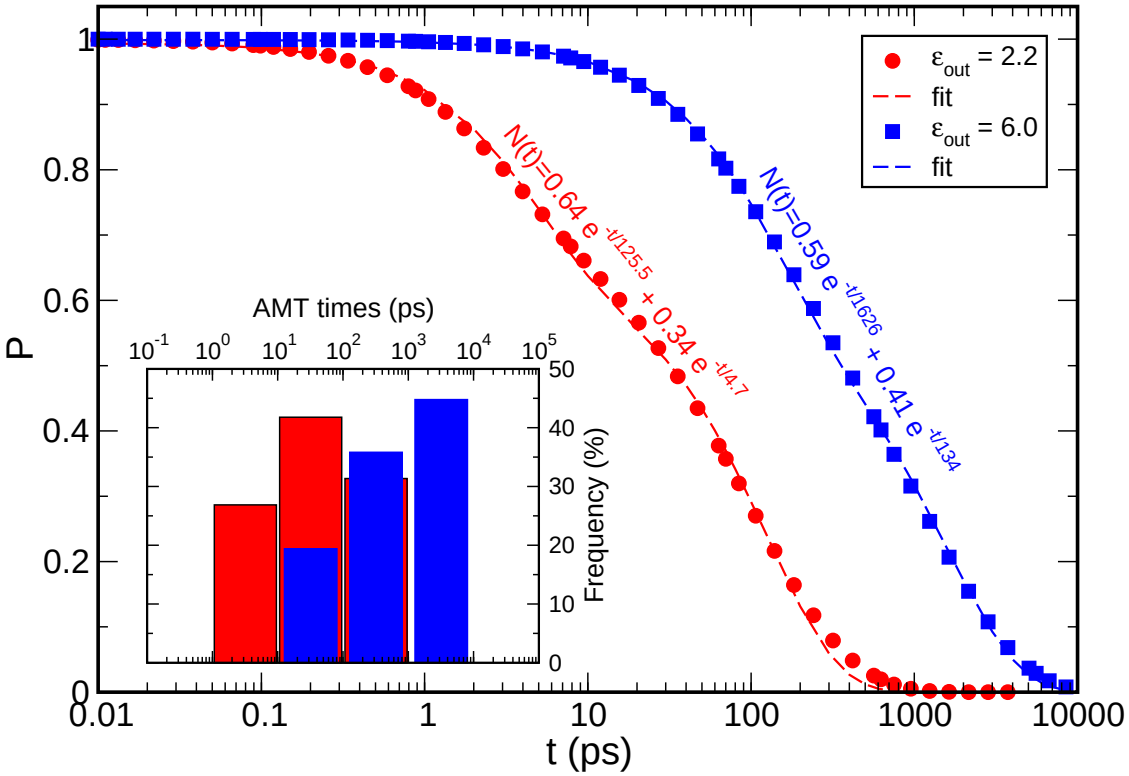

Figure 3: Theoretical population decay curves calculated for CdTe CQDs with $R = 2.3$ nm in two different dielectric environments ($\epsilon_{\text{out}} = 2.2$, solid red circles, and 6, solid blue squares), together with their bi-exponential fits (dashed lines). The equation of the bi-exponential functions are shown along the relative curves. Inset: the distribution of calculated AMT times in the two environments (the color coding is the same as in the main frame: $\epsilon_{\text{out}} = 2.2$, red bars, and $\epsilon_{\text{out}} = 6$, blue bars). The width of the blue bars has been reduced for clarity.

depopulation of the $1S_e$ electron state.[4,5,30] Could this have been due to the *excitation* of the electron following the AMT of the *hole*, rather than to electron *trapping*? Some support for this intriguing hypothesis may be found in the reported observation of a broad photoinduced absorption (PIA) feature below the band gap: Indeed, although this feature was attributed in *CdSe* CQDs to the presence of trapped charges,[26–28] very recent three pulse femtosecond spectroscopic experiments in *PbSe* CQDs[29] associated it instead with excited state absorption (i.e., with the presence of hot excitons). Is it therefore possible that the below-band-edge induced absorption observed by Boehme *et al.* in CQD dispersions featuring low PL quantum yield and fast trapping, could be evidence of the presence of (i) the electron in excited states above the conduction band edge, and (ii) the

trapped hole?

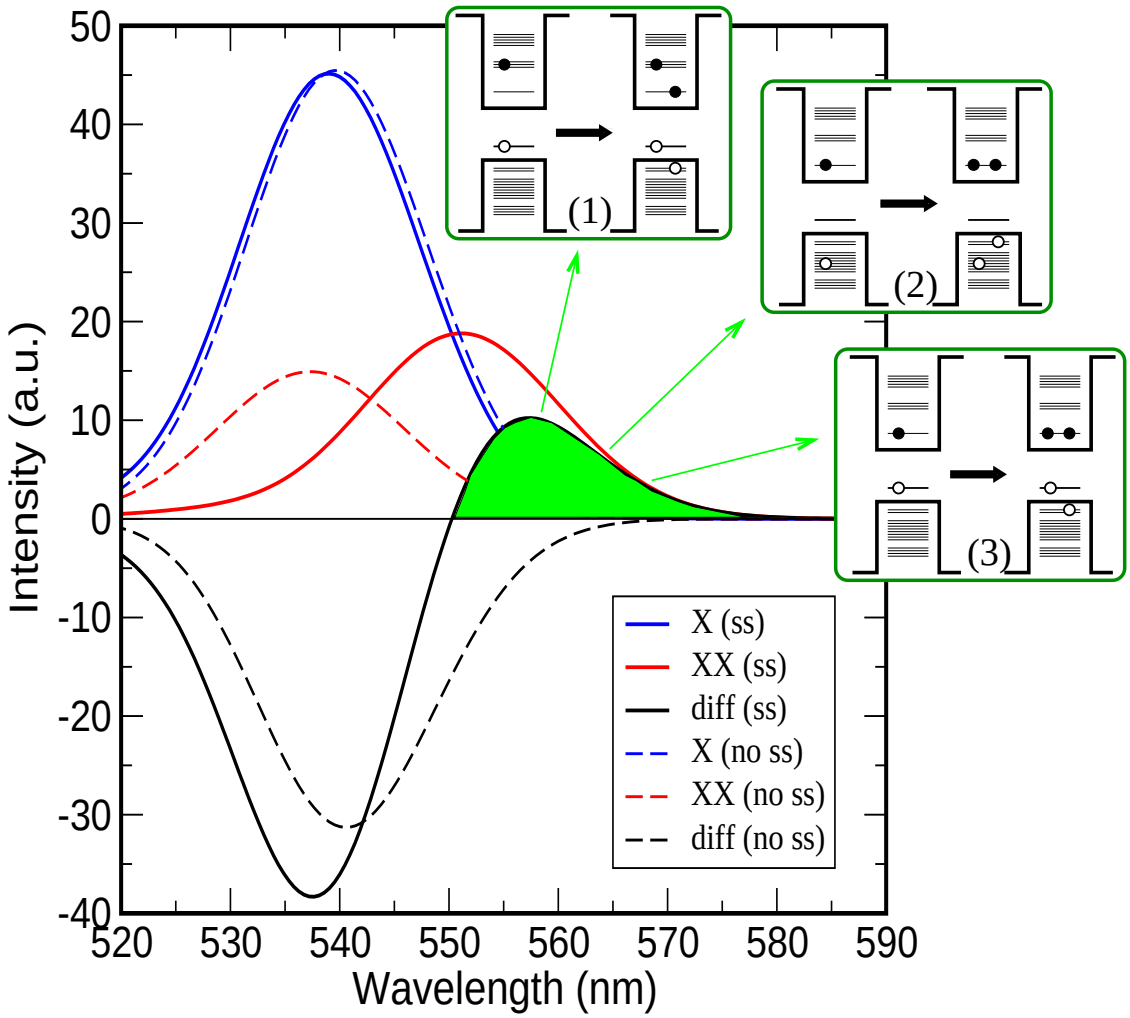

Figure 4: Theoretical absorption curves and transients calculated, for different exciton populations (0 electrons and 0 holes, blue lines; 1 electron and 1 hole, red lines), for a CdTe CQD with $R = 1.1$ nm, both in the presence (solid lines) and in the absence (dashed lines) of a hole trap state (ss=surface state). The PIA feature at energies below the band gap is highlighted in green. The three cartoons represent the different transitions contributing to this feature.

In order to verify if that may be the case, we calculated the absorption spectra for a $R = 1.1$ nm CdTe CQD populated with 0 and 1 excitons, in the presence and in the absence of a hole trap state. The results are presented in Figure 4 [c], where the solid lines refer to the former case (ss=surface state) and the dashed lines to the latter (no ss). We find that:

[c]The theoretical PIA is not as broad as in the experimental case,[17] as, being obtained for a single dot and, most importantly, for a single trap state, does not include the broadening effects due to the energy distribution of the different types of traps (see Figure 1), and, to a lesser extent, to size dispersion.

(i) there is no PIA in the absence of a surface-trapped charge; (ii) in the presence of a trap state, there are indeed two extra transitions contributing to the PIA, in addition to $|h_{ss},e_1\rangle \rightarrow |h_{ss},h_{1,2},e_1,e_1\rangle$,(panel (3) in Figure 4, which involves the presence of a trapped *hole* and a CB electron): (1) $|h_{ss},e_{p_j}\rangle \rightarrow |h_{ss},h_{1,2},e_{p_j},e_1\rangle$, where the initial state is precisely the final state of the Auger-mediated trapping transition for this specific trap ($|h_1,e_1\rangle \rightarrow |h_{ss},e_{p_j}\rangle$, see Figure 1); (2) $|h_n,e_1\rangle \rightarrow |h_n,h_{1,2},e_1,e_1\rangle$, where the initial states are exactly the final states of the Auger-mediated electron cooling from the p-like states to the CBM ($|h_1,e_{p_j}\rangle \rightarrow |h_n,e_1\rangle$). These results are therefore consistent with the hypothesis of an AMT of the hole through the excitation of the electron. This strong link between the presence of excited electrons and efficient trapping in the dots (i.e., evidence of AMT of the hole), is further supported by the fact that the magnitude of the PIA was found to be related to a short lifetime of the $1S_{3/2}1S_e$ bleach.[17]

Our results also suggest that following AMT of the hole, the excited electron could undergo fast Auger-assisted decay, restoring the electron population of the $1S_e$ state (we, however, calculate a 1 ps lifetimes for this process versus a much faster hole trapping time of 300 fs, for the trap considered in Figure 4), and leading to a configuration with an excited hole and a CBM electron (the initial state in panel (2) of Figure 4). Owing to the fast hole relaxation times, this would ultimately result in a configuration with a cold delocalized exciton (a VBM hole and a CBM electron), leading to a persistence of the absorption bleach, in contrast with experiment.

In conclusion, we believe that the above results, although inconclusive, suggest that hole trapping may have contributed to the behavior observed by Boehme *et al.* in dispersions of CdTe CQDs. At the same time, as mentioned above, the results obtained here are not trivially generalisable to densely packed CQD *films*, due to the higher complexity of the dot's environment in these systems.

Other experimental groups reported longer lifetimes for the two components of the bi-exponential fit: Patra *et al.*[18] found fast components (τ_f) of the order of a few hundreds

of ps and slow components (τ_s) in the ns range. Similarly Espinobarro-Velazquez *et al.*,[19] extracted values for τ_f bordering the ns range and $2 < \tau_s < 10$ ns. So the questions arise of (i) whether these components originate from the trapping of the same kind of charge carrier responsible for the sub-ns decays observed elsewhere,[17] and, if so, (ii) why they are orders of magnitude larger.

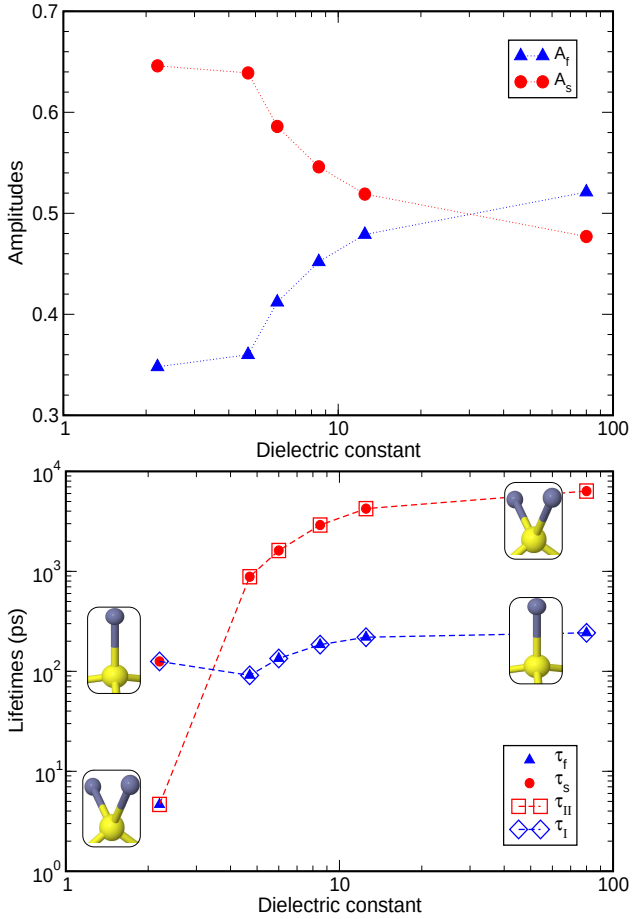

Figure 5: Variation, as a function of the dielectric constant of the dot environment, of the fast (solid blue triangles) and slow (solid red circles) components [amplitudes, (a), and lifetimes, (b)] extracted from a bi-exponential fit to the theoretical population decay of CdTe CQDs with $R = 2.3$ nm. Lines are a guide to the eye. The dashed lines in (b) connect lifetimes relative to type-I (empty blue diamonds) and type-II (empty red squares) traps, also shown by the cartoons.

We find the calculated trapping times to be crucially sensitive to the specific CQD environment. This characteristic is particularly evident in Figure 3, where a change in the dielectric constant of the dot matrix ϵ_{out} from 2.2 (i.e., a common solvent, like toluene, or a

common capping group, like TOPO), to 6 (i.e., a common oxide like CdO) leads to orders of magnitude increase of the AMT lifetimes. For a dot with $R = 2.3$ nm, the formation of CdO on its surface would bring the slow component of the bi-exponential fit into the ns range and increase τ_f by about two orders of magnitude (see Figure 3), in agreement with experiment.[18] Interestingly we find that it is the lifetime relative to the efficient traps, obtained from an unsaturated bond which is part of a pair (II) of dangling bonds on the same Te atom, (τ_{II}) that undergoes the largest variation (about 3 orders of magnitude), becoming the slower component (τ_s) in environments with a higher dielectric constant (see Figure 5). What is labelled as the slow component in low-dielectric environments ($\epsilon_{\mathrm{out}} = 2.2$), associated with the less efficient traps originating from a single (I) dangling bond (τ_{I}), is instead little affected by the increase of dielectric constant of the environment and becomes the fast component for high values of ϵ_{out}. This effect is also shown in Figure 6a where the AMT times of a type I and a type II trap are compared in different dielectric environments [the lifetimes are plotted as a function of $\delta\Delta E$ to account for possible variations in the trap depth ΔE_v^{ht} (or, equivalently, - however with the opposite sign - in the calculated value of ΔE_c^{sj}, see Figure 1), around its calculated position ($\delta\Delta E = 0$), due to size/shape anisotropy in the sample and/or external causes (such as local electric fields)]: focusing on the lifetimes at $\delta\Delta E = 0$, it is apparent that the most efficient (type II) trap in a low dielectric environment becomes the least efficient for $\epsilon_{\mathrm{out}} = 6$ and *vice versa* for the type I trap.

The origins of this behavior can be understood by decomposing the expression for the trapping rate (see (Eq. (1)) in the Method section below) into AMT coupling (numerator) and energy conservation (denominator) and analyzing them separately: the matrix elements relative to AMT transitions to the two traps (the numerator of (Eq. (1))) are found to be very similar, for both dielectric environments. This is clearly shown in Figure 6b, where these matrix elements are displayed as a function of the energy difference between the initial excitonic states $|i_n\rangle$ and the energetically lowermost final excitonic state $|f_1\rangle$

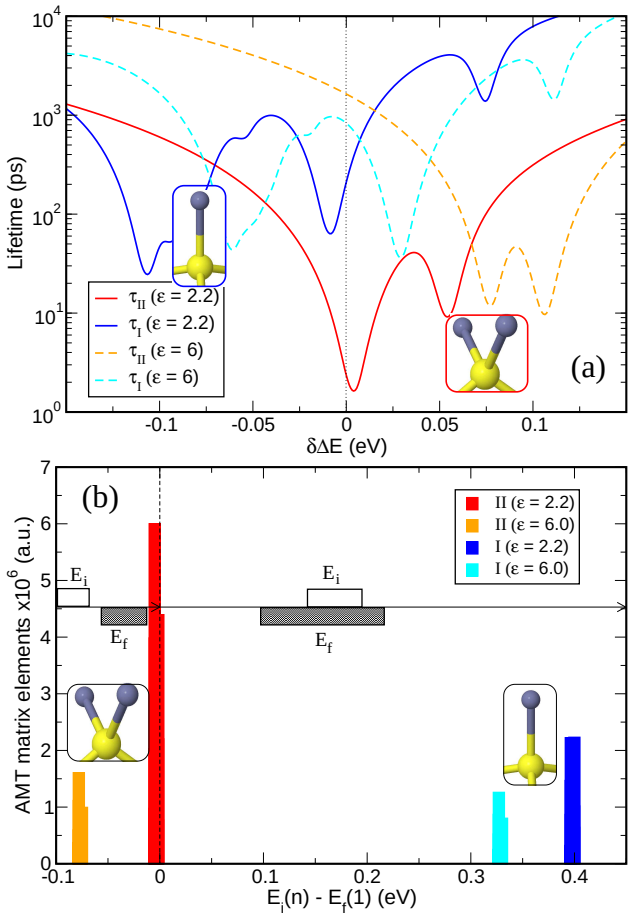

Figure 6: AMT times (a) and matrix elements (b), calculated for transitions to a selected type-I and type-II trap on the surface of a CdTe CQD with $R = 2.3$ nm. The trapping times (a) are plotted as a function of $\delta\Delta E$ ($\Delta E = \Delta E_v^{ht}$ or $\Delta E = \Delta E_c^{sj}$) to account for possible variations in the trap depth ΔE_v^{ht} (or, equivalently, - however with the opposite sign - in the calculated value of ΔE_c^{sj}, see Figure 1), around its calculated position ($\delta\Delta E = 0$), due to size/shape anisotropy in the sample and/or external causes (such as local electric fields). The matrix elements (b) are displayed as a function of the energy difference between the initial excitonic state $E_i(n)$ and the lowermost final excitonic state $E_f(1)$. The different regimes corresponding to the positive and negative values of $E_i(n) - E_f(1)$ are schematically depicted by the cartoons.

(the left-hand side of the gray box in the cartoon). When this difference is negative (as it is the case for the type II trap and $\epsilon_{\text{out}} = 6$), energy is not conserved in the transition, as the energy of all initial states is lower than that in the final states. Conservation of energy can only be attained for positive values of $E_i(n) - E_f(1) < \varepsilon_0$, where $\varepsilon_0 = E_f(\text{last}) - E_f(1)$ is the spread of the final state energies ($\varepsilon_0 \approx 0.45$ eV for the type I trap), in which case initial and final states *may* be in resonance, unless there are gaps within the final states manifold coinciding with the energetic position of the initial states. This is the case for the type I trap for both $\epsilon_{\text{out}} = 2.2$ and 6, as shown in Figure 6a, where the lifetime reaches its minimum values away from $\delta\Delta E = 0$. The trapping efficiencies for different dielectric environments are therefore mostly dictated by energy conservation (i.e., the denominator of (Eq. (1))): trap II is efficient for $\epsilon_{\text{out}} = 2.2$ when Auger coupling is strongest (the matrix element assumes its largest value) and the transition conserves energy (the difference between the energies of initial and final states is close to zero). An increase in the dielectric constant of the environment leads both to a reduction (by a factor of about 4) of the matrix elements' magnitude and to significant energy dephasing (about 80 meV) in the trapping transition. In contrast, in the case of the type I trap the coupling strength is less affected by a change in the dielectric environment (it decreases by a factor of about 2 with increasing ϵ_{out}), and although the energy dephasing looks similar to the one occurring for the type-II trap, the energy range of the initial states still overlaps that of the final states. This energy landscape creates a series of closely-spaced resonances that prevent large variations in τ_I even when energy is not exactly conserved in the transition. In the case of a type-II trap, instead, the combination of (i) non overlapping initial and final energy ranges and (ii) a narrow energy range for the final states leads to a monotonically increasing τ_{II} away from resonance, hence large variations even for relatively small energy dephasings.

In order to translate this behavior into experimentally measurable quantities, in Figure 5 we plot the lifetimes (τ_f and τ_s), and the relative amplitudes (A_f and A_s), of the two components obtained from the bi-exponential fits to the theoretical population decays cal-

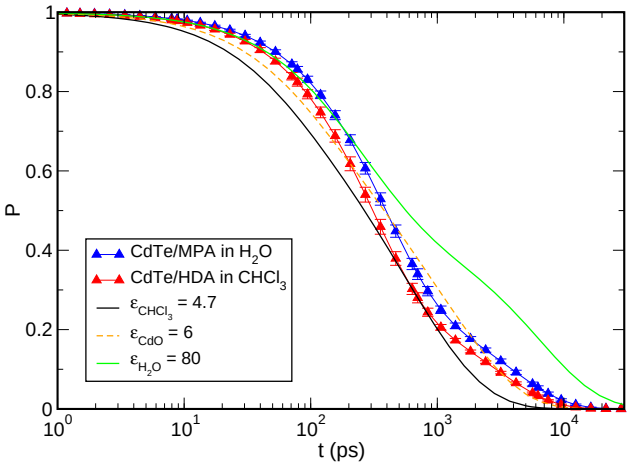

Figure 7: Comparison between experimental[18] (solid symbols and lines) and theoretical (lines) population decays. The experimental data refer to CdTe CQD samples with different capping agents in different media (Hexadecylamine, HDA, in $CHCl_3$ - solid red triangles - and mercaptopropionic acid, MPA, in H_2O - solid blue triangles). The theoretical curves are calculated for CdTe dots with $R = 2.3$ nm in different dielectric environments: $\epsilon_{\text{out}} = 4.7$ ($CHCl_3$, black solid line), 6 (∼CdO, orange dashed line), and 80 (H_2O, green solid line).

culated for a wide range of values of the dielectric constant ϵ_{out} of the dot environment. It is worth noticing that the amplitudes of the two components follow opposite trends with increasing ϵ_{out}: whilst A_f increases with ϵ_{out}, the opposite is true for A_s. A similar trend for the amplitudes of the two non-radiative components was indeed observed by Espinobarro-Velazquez *et al.*[19] in CdTe CQDs as a function of air exposure. Based on Figure 5, we therefore suggest that this effect could be associated with the progressive increase in the dielectric environment of the CQDs, consistent with the formation of a native oxide (CdO or $CdTeO_3$) on the surface, following oxygen exposure.

Most interestingly, Figure 5 also establishes a strong link between the presence of type-I traps and the observation of a sub-ns component in the fluorescence decay curves of CdTe CQDs in the size range considered here. This connection suggests that the absence from experimental data of trapping times in such a range should imply efficient passivation of type-I traps in the sample.

The experimental population decays obtained using amplitudes and lifetimes rela-

tive to the non-radiative components [d] extracted by Patra *et al.*[18] from CdTe CQD samples with different capping agents (Hexadecylamine, HDA, and mercaptopropionic acid MPA), and in different media ($CHCl_3$ and H_2O) are compared with the theoretical curves calculated with $\epsilon_{out} = 4.7$ ($CHCl_3$), 6 ($\sim$CdO), and 80 (H_2O) in Figure 7 (the values at zero irradiation time are chosen here to remove all light-induced effects discussed in ref.[18]). This comparison seems to suggest a dot environment with a dielectric constant larger than that of $CHCl_3$. The best agreement is achieved with a curve consistent with the presence of an oxide (or a shell of some other inorganic material) on the dot surface. However, it should be pointed out that, considering the difference in size between the experimental samples and the theoretical dots, it is difficult to extract from the figure an estimate for the value of the dielectric constant of the dot environment.

Conclusions

In summary, we have shown that the different features observed in the non-radiative decay of dispersions of CdTe CQDs with different surface terminations can be explained in terms of the trapping of the hole at unsaturated Te bonds at the dot surface *via* an Auger-mediated mechanism. The fast and slow components extracted from a bi-exponential fit to our calculated population decay (obtained considering the contribution of up to 268 surface traps) reproduce the observed behavior of the trapping times as a function of size, and of both trapping times and amplitudes as a function of air exposure. The latter effect is explained in terms of a modification of the dielectric environment of the dot caused by the progressive formation on the surface of a native oxide (CdO or $CdTeO_3$), with increasing air exposure time, whose dielectric constant is higher than that of the capping group. The behavior of these components is analyzed in detail as a function of the di-

[d] Out of the three components extracted from the triexponential fit by Patra *et al.*, one (number 2 in Table 1 of ref.[18]) has a lifetime magnitude compatible with the radiative decay time[31] and an amplitude that follows the observed photoluminescence intensity. We therefore attribute it to radiative decay and associate the remaining two components (1 and 3) with the (slow and fast) non-radiative components.

electric environment of the dot, which is found to be a crucial parameter determining the magnitude of the trapping times through a modification of both the Auger coupling and the energetics of the transitions. The two components are associated with the trapping to dangling bonds that are either single (I) or part of a pair (II) on the same Te atom (in which case the other bond is fully saturated). These two kinds of traps are found to have distinct size-independent energies in the gap, fixed with respect to the VBM in bulk CdTe, whose calculated position in the lower part of the energy gap is consistent with observation. Based on the calculated behavior of the transfer times to traps I (totalling 148 on the surface of a CdTe dot with $R = 2.3$ nm) and II (totalling 120) as a function of dielectric environment, and as a function of the energy landscape of initial and final states, we expect that a sub-nanosecond component should always be observed in the PL decay curves of CdTe CQDs in the size range considered here, consistently with most experimental findings so far. The absence of such a fast component would imply the suppression or deactivation, possibly due to passivation, of type I traps. The hypothesis of the existence of a majority of type II traps in some samples is consistent with the decreased efficiency of passivating two dangling bonds (compared to a single one) on a single atom, due to, e.g., steric hindrance effects in the case of organic ligands, or to electrostatic interactions in the case of ionic passivation.

Method

Within the semi-empirical pseudopotential approach, the CQD is built with bulk-like structure, starting from its constituent atoms, up to the desired radius. This procedure yields surface atoms with unsaturated bonds. Atoms with only one (saturated) bond are removed, as they are unstable for dissociation,[32] leaving on the surface only atoms with one or two missing bonds. These surface dangling bonds are passivated by pseudo-hydrogenic, short-range potentials with Gaussian form. A hole surface trap state was

created by removing a single passivant from a surface anion. The single-particle energies and wave functions were calculated using the plane-wave semiempirical pseudopotential method described in Reference,[25] including spin-orbit coupling, and excitonic effects were accounted for *via* a configuration interaction scheme.[33] (More detailed information on the theoretical method can be found in our previous work[13]).

AMT times were calculated using Fermi's Golden Rule according to[34]

$$(\tau_{\mathrm{AMT}})_i^{-1} = \frac{\Gamma}{\hbar} \sum_n \frac{| < i|\Delta H|f_n > |^2}{(E_{f_n} - E_i)^2 + (\Gamma/2)^2}. \quad (1)$$

where $|i>$ and $|f_n>$ are the initial (delocalised) and final (trapped) excitonic states (see Figure 1), E_i and E_{f_n} are their energies, ΔH is the Coulomb interaction and $\hbar/\Gamma$ is the lifetime of the final states.

Acknowledgement

M.C. gratefully acknowledges financial support from the Royal Society under the URF scheme.

References

1. Jones, M.; Lo, S. S.; Scholes, G. D. Quantitative Modelling of the Role of Surface Traps in CdSe/CdS/ZnS Nanocrystal Photoluminescence Decay Dynamics. *Proc. Nat. Acad. Sci.* **2009**, *106*, 3011-3016.

2. Kern, S. J.; Sahu, K.; Berg, M. A. Heterogeneity of the Electron Trapping Kinetics in CdSe Nanoparticles. *Nano Lett.* **2011**, *11* 3493-3498.

3. Knowles, K. E.; McArthur, E. A.; Weiss, E. A. A Multi-Timescale Map of Radiative and Nonradiative Decay Pathways for Excitons in CdSe Quantum Dots. *ACS Nano*, **2011**, *5*, 2026.

4. Kambhampati, P. Unravelling the Structure and Dynamics of Excitons in Semiconductor Quantum Dots. *Acc. Chem. Res.* **2011**, *44*, 1-13.

5. Kambhampati, P. Hot Exciton Relaxation Dynamics In Semiconductor Quantum Dots: Radiationless Transitions on the Nanoscale. *J. Phys. Chem. C* **2011**, *115*, 22089-22109.

6. Kambhampati, P. On the Kinetics and Thermodynamics of Excitons at the Surface of Semiconductor Nanocrystals: Are There Surface Excitons? *Chem. Phys.* **2015**, *446*, 92-117.

7. Zillner, E.; Fengler, S.; Niyamakom, P.; Rauscher, F.; Kohler, K.; Dittrich, T. Role of Ligand Exchange at CdSe Quantum Dot Layers for Charge Separation. *J. Phys. Chem. C* **2012**, *116*, 16747-16754.

8. Avidan, A.; Pinkas, I.; Oron, D. How Quickly Does a Hole Relax into an Engineered Defect State in CdSe Quantum Dots. *ACS Nano* **2012**, *6*, 3063-3069.

9. Guyot-Sionnest, P.; Wehrenberg, B.; Yu, D. Intraband Relaxation in CdSe Nanocrystals and the Strong Influence of the Surface Ligands. *J. Chem. Phys.* **2005**, *123*, 074709-1-074709-7.

10. Qin, W.; Guyot-Sionnest, P. Evidence for the Role of Holes in Blinking: Negative and Oxidized CdSe/CdS Dots. *ACS Nano* **2012**, *6*, 9125-9132.

11. Cadirci, M. *et al.* Ultrafast exciton dynamics in InAs/ZnSe nanocrystal quantum dots. *Phys. Chem. Chem. Phys.* **2012**, *14*, 15166-15172.

12. Cordones, A. A.; Leone, S. R. Mechanisms for Charge Trapping in Single Semiconductor Nanocrystals Probed by Fluorescence Blinking. *Chem. Soc. Rev.* **2013**, *42*, 3209-3221.

13. Gomez-Campos, F. M.; Califano, M. Hole Surface Trapping in CdSe Nanocrystals:

Dynamics, Rate Fluctuations, and Implications for Blinking. *Nano Lett.* **2012**, *12*, 4508-4517.

14. Califano, M.; Gomez-Campos, F. M. Universal Trapping Mechanism in Semiconductor Nanocrystals. *Nano Lett.* **2013**, *13*, 2047-2052.

15. Zhu, H.; Yang, Y.; Hyeon-Deuk, K.; Califano, M.; Song, N.; Wang, Y.; Zhang, W.; Prezhdo, O. V.; Lian, T. Auger-Assisted Electron Transfer from Photoexcited Semiconductor Quantum Dots. *Nano Lett.* **2014**, *14*,1263-1269

16. Voznyy, O; Sargent, E. H. Atomistic Model of Fluorescence Intermittency of Colloidal Quantum Dots, *Phys. Rev. Lett.* **2014**, *112*, 157401.

17. Boehme, S. C.; Walvis, T. A.; Infante, I.; Grozema, F.C.; Vanmaekelbergh, D.; Siebbeles, L.; Houtepen, A. Electrochemical Control over Photoinduced Electron Transfer and Trapping in CdSe-CdTe Quantum-Dot Solids. J. *ACS Nano* **2014**, *7*, 7067-7077.

18. Patra, S.; Samanta, A. Effect of Capping Agent and Medium on Light-Induced Variation of the Luminescence Properties of CdTe Quantum Dots: A Study Based on Fluorescence Correlation Spectroscopy, Steady State and Time-Resolved Fluorescence Techniques. *J. Phys. Chem. C* **2014**, *118*, 18187-18196.

19. Espinobarro-Velazquez, D.; Leontiadou, M. A.; Page, R. C.; Califano, M.; O'Brien, P.; Binks, D. Effect of Chloride Passivation on Recombination Dynamics in CdTe Colloidal Quantum Dots. *Chem. Phys. Chem.* **2015** *DOI:10.1002/cphc.201402753* .

20. Gaponik, N.; Talapin, D. V.; Rogach, A. L.; Hoppe, K.; Shevchenko, E. V.; Kornowski, A.; Eychmüller, A.; Weller, H. Thiol-Capping of CdTe Nanocrystals: An Alternative to Organometallic Synthetic Routes. *J. Phys. Chem. B* **2002**, *106*, 7177-7185.

21. Glozman, A.; Lifshitz, E.; Hoppe, K.; Rogach, A. L.; Weller, H.; Eychmüller, A. Opti-

cally Detected Magnetic Resonance of Thiol-Capped CdTe Nanocrystals. *Isr. J. Chem.* **2001**, *41*, 39-44.

22. Poznyak, S. K.; Osipovich, N. P.; Shavel, A.; Talapin, D. V.; Gao, M.; Eychmüller, A.; Gaponik, N. Size-Dependent Electrochemical Behavior of Thiol-Capped CdTe Nanocrystals in Aqueous Solution. *J. Phys. Chem. B* **2005**, *109*, 1094-1100.

23. Borchert, H.; Talapin, D. V.; Gaponik, N.; McGinley, C.; Adam, S.; Lobo, A.; Möller, T.; Weller, H. Relations between the Photoluminescence Efficiency of CdTe Nanocrystals and Their Surface Properties Revealed by Synchrotron XPS. *J. Phys. Chem. B* **2003**, *107*, 9662.

24. Frantsuzov, P. A.; Marcus, R. A. Explanation of Quantum Dot Blinking Without the Long-Lived Trap Hypothesis. *Phys. Rev. B* **2005**, *72*, 155321.

25. Wang, L.-W.; Zunger, A. Local-Density-Derived Semiempirical Pseudopotentials. *Phys. Rev. B* **1995**, *51*, 17 398.

26. Malko, A. V.; Mikhailovsky, A. A.; Petruska, M. A.; Hollingsworth, J. A.; Klimov, V. I. Interplay between Optical Gain and Photoinduced Absorption in CdSe Nanocrystals. *J. Phys. Chem. B* **2004**, *108*, 5250-5255.

27. McArthur, E. A.; Morris-Cohen, A. J.; Knowles, K. E.; Weiss, E. A. Charge Carrier Resolved Relaxation of the First Excitonic State in CdSe Quantum Dots Probed with Near-Infrared Transient Absorption Spectroscopy. *J. Phys. Chem. B* **2010**, *114*, 14514-14520.

28. Saari, J. I.; Dias, E. A.; Reifsnyder, D.; Krause, M. M.; Walsh, B. R.; Murray, C. B.; Kambhampati, P. Ultrafast Electron Trapping at the Surface of Semiconductor Nanocrystals: Excitonic and Biexcitonic Processes. *J. Phys. Chem. B* **2012**, *117*, 4412-4421.

29. Gdor, I; Yanover, D.; Yang, C.; Shapiro, A.; Lifshitz, E.; Ruhman, S. Three Pulse Femtosecond Spectroscopy of PbSe Nanocrystals; 1S Bleach Nonlinearity and Sub Band-Edge Excited State Absorption Assignment. (unpublished).

30. Klimov, V. I. Optical Nonlinearities and Ultrafast Carrier Dynamics in Semiconductor Nanocrystals. *J. Phys. Chem. B* **2000**, *104*, 6112-6123.

31. de Mello Donegá, C.; Koole, R. Size Dependence of the Spontaneous Emission Rate and Absorption Cross Section of CdSe and CdTe Quantum Dots.*J. Phys. Chem. C* **2009**, *113*, 6511-6520.

32. Kilina, S.; Ivanov, S.; Tretiak, S. Effect of Surface Ligands on Optical and Electronic Spectra of Semiconductor Nanoclusters. *J. Am. Chem. Soc.* **2009**, *131*, 7717-7726.

33. Franceschetti, A.; Fu, H.; Wang, L.-W. & Zunger, A. Many-body pseudopotential theory of excitons in InP and CdSe quantum dots. *Phys. Rev. B* **1999**, *60*, 1819-1829.

34. Wang, L.-W.; Califano, M.; Zunger, A.; Franceschetti, A. Pseudopotential Theory of Auger Processes in CdSe Quantum Dots. *Phys. Rev. Lett.* **2003**, *91*, 056404.